Influence of End Group and Surface Structure on the Current−Voltage Characteristics of Alkanethiol Monolayers on Au(111)†

Jian-guo Wang* and Annabella Selloni*

Department of Chemistry, Princeton University, Princeton, New Jersey 08540

Received: July 25, 2007; In Final Form: September 24, 2007

We present density functional theory calculations of the electronic structure and tunneling characteristics of alkanethiolate monolayers on Au(111). We systematically analyze $\sqrt{3} \times \sqrt{3}$ full coverage monolayers of $SC_6H_{12}X$ molecules with different terminal groups, X = CH_3, NH_2, SH, OH, COOH, OCH_3, on defect-free ("perfect") Au(111). We also study the influence of the surface−molecule bonding structure by comparing the properties of monolayers of $SC_6H_{12}CH_3$ molecules on the perfect surface and on Au(111) surfaces with vacancies or adatoms. The tunneling currents (I) through the adsorbed monolayers with a single chemical contact have been calculated within the Tersoff−Hamann approach for voltages between −1 and +1 V. Computed currents are found to depend linearly on V at low voltage, with typical values of ∼60 and 150 pA/molecule at 0.2 and 0.5 V, respectively, in good agreement with several experimental data. Computed tunneling currents show also a significant dependence on both the terminal group X and the surface structure. In particular, in order of decreasing intensities, currents for the different end groups are $NH_2 \approx SH > CH_3 > OH > OCH_3 > COOH$. The relationships between the tunneling current, the work function of the surface + SAM, and the lineup of the HOMO with respect to the Fermi energy of the metal surface are examined.

Introduction

The challenge of understanding electron transport in molecules and molecular monolayers has motivated numerous fundamental investigations of electrode−molecule−electrode junctions over the last several years.[1−10] The main goal was to determine how the current through the junction is affected by the structure and electronic properties of the molecules and by their contacts to the electrodes. In particular, a great deal of theoretical work has focused on symmetric molecular junctions in which a single molecule is chemically bonded to two identical metal electrodes.[11−14] On the other hand, experimental studies are frequently based on scanning tunneling microscopy (STM) or conductive-probe atomic force microscopy (CP-AFM) measurements of the current−voltage ($I-V$) characteristics of self-assembled monolayers (SAMs) of elongated organic molecules sandwiched between two nonequivalent electrodes:[5,7,8,10,15,16] the molecules are chemisorbed through an appropriate head group on a metal surface, representing one of the electrodes, while the other contact, which may or may not involve chemical bonding, is formed through the STM or CP-AFM tip.

In this study, we tried to gain new insights into the tunneling properties of metal−SAM−tip junctions with a single chemical contact, by performing first principles calculations on the effect of the molecular end group and surface−molecule bonding geometry on the $I-V$ characteristics of $\sqrt{3} \times \sqrt{3}$ full coverage monolayers of alkanethiols on Au(111). Recent work by our group[16,17] indicates that for such junctions, and for SAMs of short to intermediate length molecules, a simple approach based on Tersoff−Hamann's[18] theory of the scanning tunneling microscope can quite satisfactorily describe the differences in tunneling properties of structurally similar molecules. For instance, differences between the computed $I-V$ characteristics for $SC_5H_{10}CH_3$ and $SC_5H_{10}CF_3$ monolayers on Au(111)[17] were found to qualitatively agree with STM measurements on SAMs of CH_3 and CF_3 terminated decanethiols.[15] In the present work, we use again the simple Tersoff−Hamann approach to perform a more systematic study of the $I-V$ characteristics of prototype SAMs of intermediate chain length alkanethiols on Au(111). To determine how the tunneling current depends on the molecular properties, we consider $SC_6H_{12}X$ monolayers, with X = CH_3, SH, OH, NH_2, OCH_3, COOH (see Figure 1). In addition, we investigate the influence of the metal−molecule interface on the $I-V$ characteristics by carrying out calculations for both defect-free Au(111) and defected surfaces with vacancies and adatoms. The different end groups are found to affect the $I-V$ tunneling characteristics as well as the work function of the surface + SAM systems. Similarly, the structure of the metal substrate affects the tunneling current as well as the alignment between the molecular levels and the Fermi energy of the metal. Correlations between the different properties are identified.

Calculations

The calculations were carried out within density functional theory (DFT), using the gradient-corrected PW91 functional.[19] The neglect of van der Waals (vdW) interactions, implicit in the use of this standard DFT approach, is expected to be a reasonable approximation for the intermediate length ($n = 6$) chains considered in this work: for instance, recent quantum mechanical/molecular mechanical calculations have found that vdW contributions to the stability of alkanethiol monolayers are significant but not decisive for chains with $n = 10$ and decrease steadily, becoming negligible for $n = 4$ chains.[20] Ultrasoft pseudo-potentials[21] were used to describe electron−ion interactions, with plane-wave basis set cutoffs of 25 and 200 Ry for the smooth part of the electron wave functions and

† Part of the "Giacinto Scoles Festschrift".

* Corresponding authors. E-mail: (J.-g.W.) jianguow@princeton.edu and (A.S.) aselloni@princeton.edu.

10.1021/jp075875f CCC: $37.00
Published on Web 11/13/2007

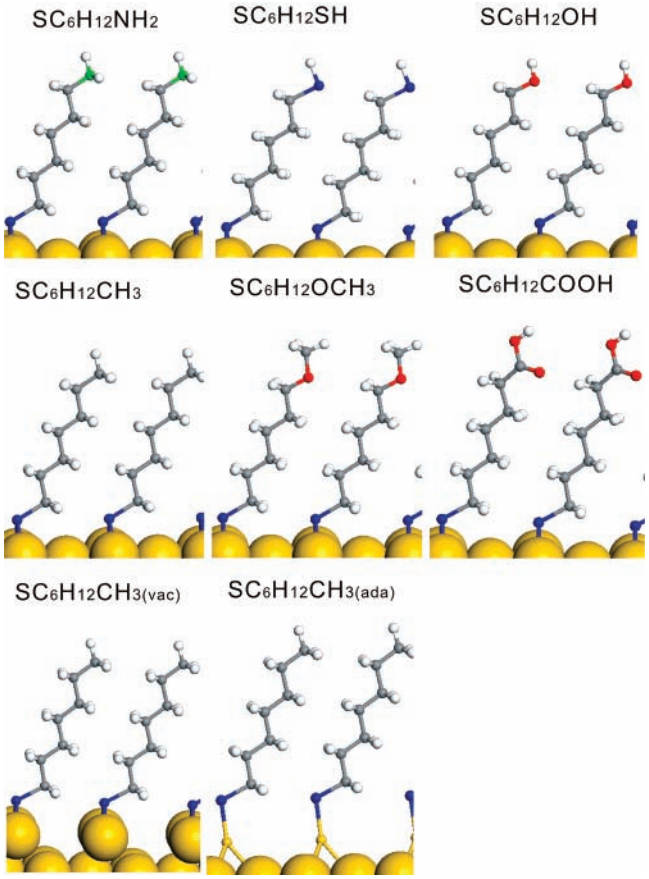

Figure 1. Optimized structures of $SC_6H_{12}X$ (X = NH_2, SH, OH, CH_3, OCH_3, COOH) on perfect Au(111) and $SC_6H_{12}CH_3$ on Au(111) with vacancies (vac) and adatoms (ada).

augmented electron density, respectively. Au(111) surfaces were modeled using a repeated slab geometry, with slabs of four layers and a separation of ~20 A between successive slabs. Test calculations showed that the results do not change significantly by increasing the number of Au layers or the distance between slabs. The clean Au(111) surface exhibits a $\sqrt{3} \times 23$ reconstruction,[22] but it is known that this is lifted in the presence of a $\sqrt{3} \times \sqrt{3}$ alkanethiol monolayer at saturation coverage.[23] We thus considered a bulk terminated surface with a $\sqrt{3} \times \sqrt{3}$ surface unit cell containing three Au atoms per layer and one adsorbed $SC_6H_{12}X$ molecule on one side only of the slab. In the case of defected surfaces, one surface vacancy or one Au adatom per unit cell is also present. The Brillouin zone was sampled with 48 special *k*-points. In the geometry optimizations, the adsorbed molecule and the topmost two layers of the Au(111) slab were relaxed until each component of the residual force on each atom was smaller than 0.03 eV/Å.

To calculate $I-V$ characteristics, we used the expression[16,17]

$$I \approx e v_{\mathrm{eff}} \int_A \mathrm{d}x\, \mathrm{d}y \int_{E_F}^{E_F+eV} \mathrm{d}E \rho_s(x,y,z_0 :\ E)$$

where ρ_s (x, E) is the local density of states (LDOS) of the Au(111)/SAM system at zero applied bias (implying that V must be small with respect to the system work function); A is the contact area that we take to be equal to the surface area per molecule (thus I corresponds to the current through a single molecule); z_0 is the vertical position of the STM tip; and v_{eff} is an effective velocity of the tunneling electrons that we take to be equal to the Fermi velocity for gold. For z_0, we take a point in the vacuum gap ~2.0 Å above the apex of the molecule, where the tails of the charge density of the successive slab are negligible. Note that in the previous expression, which is based on perturbation theory,[18] the interaction of the molecule with the tip electrode is not included.

TABLE 1: Work Function Modification ($\Delta\Phi$), HOMO Energy (ΔE), Energy (E_T) of Peak in Terminal PDOS, Current per Molecule (I), and Molecular Length for SAMs of $SC_6H_{12}X$ (X = CH_3, NH_2, SH, OH, COOH, OCH_3) on Defect-Free Au(111)[a]

	$\Delta\Phi$ (eV)	ΔE (eV)	E_T (eV)	I (pA) at 0.5 V	I (pA) at 0.2 V	molecular length (Å)
$SC_6H_{12}NH_2$	−1.50	−0.85	−1.20	165	58	9.92
$SC_6H_{12}SH$	−1.00	−0.85	−1.13	151	60	10.30
$SC_6H_{12}OH$	−1.80	−0.85	−2.11	136	49	9.84
$SC_6H_{12}CH_3$	−1.05	−0.85		143	58	10.06
$SC_6H_{12}OCH_3$	−1.20	−0.85	−1.68	112	47	11.09
$SC_6H_{12}COOH$	−1.20	−0.85	−2.33	74	31	10.96
$SC_6H_{12}CH_{3(vac)}$	−1.05	−0.85		99	56	10.06
$SC_6H_{12}CH_{3(ada)}$	−0.40	−0.18		171	70	10.06

[a] For $SC_6H_{12}CH_3$, results for monolayers on Au(111) surfaces with vacancies, $SC_6H_{12}CH_{3(vac)}$, and adatoms, $SC_6H_{12}CH_{3(ada)}$, are also listed.

Results and Discussion

(a) Structure and Electronic Properties of $SC_6H_{12}X$, X = NH_2, SH, OH, CH_3, OCH_3, COOH, Monolayers on Defect-Free Au(111). The optimized structures of the investigated $SC_6H_{12}X$ monolayers on the defect-free ("perfect") Au(111) surface are shown in Figure 1. To facilitate comparisons, we have chosen geometries in which the apex atom(s) is(are) always hydrogen(s). In addition, all adsorbed molecules have approximately the same height (within 1 Å), except for the somewhat "taller" $SC_6H_{12}COOH$ and $SC_6H_{12}OCH_3$ molecules. Starting from the known case of $SC_6H_{12}CH_3$, in agreement with previous theoretical studies,[24−26] we find that the alkanethiolate sulfur head group prefers to adsorb at the bridge-fcc site, with a S−Au bond distance of ~2.49 Å. The computed height of the S head group over the Au surface is ~2.1 Å, consistent with X-ray standing wave (XSW) data[27] for the c(4 × 2) structure of decanethiols on Au(111) (note that for the c(4 × 2) structure, two inequivalent sulfur head groups occur:[27,28] our calculated height of 2.1 Å agrees with the smaller of the two values found in the XSW experiment). The tilt angle of the alkane chains, ~23°, is also consistent with experiment.[29] Since for the SAMs of the other $SC_6H_{12}X$ alkanethiolates no precise structural information is available from experiments,[30] we start from the same geometry (adsorption site, packing density, and tilt angle) of $SC_6H_{12}CH_3$ and then carry out a full structural optimization according to the procedure described in Calculations.

For each adsorbed monolayer, the work function Φ has been calculated from the energy difference between the value of the electrostatic potential in the vacuum region and the Fermi energy E_F.[17,31,32] The dipole layer arising in the vacuum gap region because of the periodic boundary conditions was subtracted. For the clean Au(111) surface, the calculated work function is $\Phi_0 = 5.30$ eV, in good agreement with the experimental value of 5.31 eV. The work function changes, $\Delta\Phi = \Phi - \Phi_0$, induced by the different monolayers with respect to clean Au(111), are given in Table 1. In all investigated cases, the SAM induces a decrease of the work function ($\Delta\Phi < 0$). End groups with a large dipole moment, such as OH and NH_2, lead to a large work function decrease, $\Delta\Phi = -1.80$ and -1.50 eV, respectively. The symmetric thiol (SH) termination gives rise to a work function change $\Delta\Phi = -1.00$ eV, very similar to the value

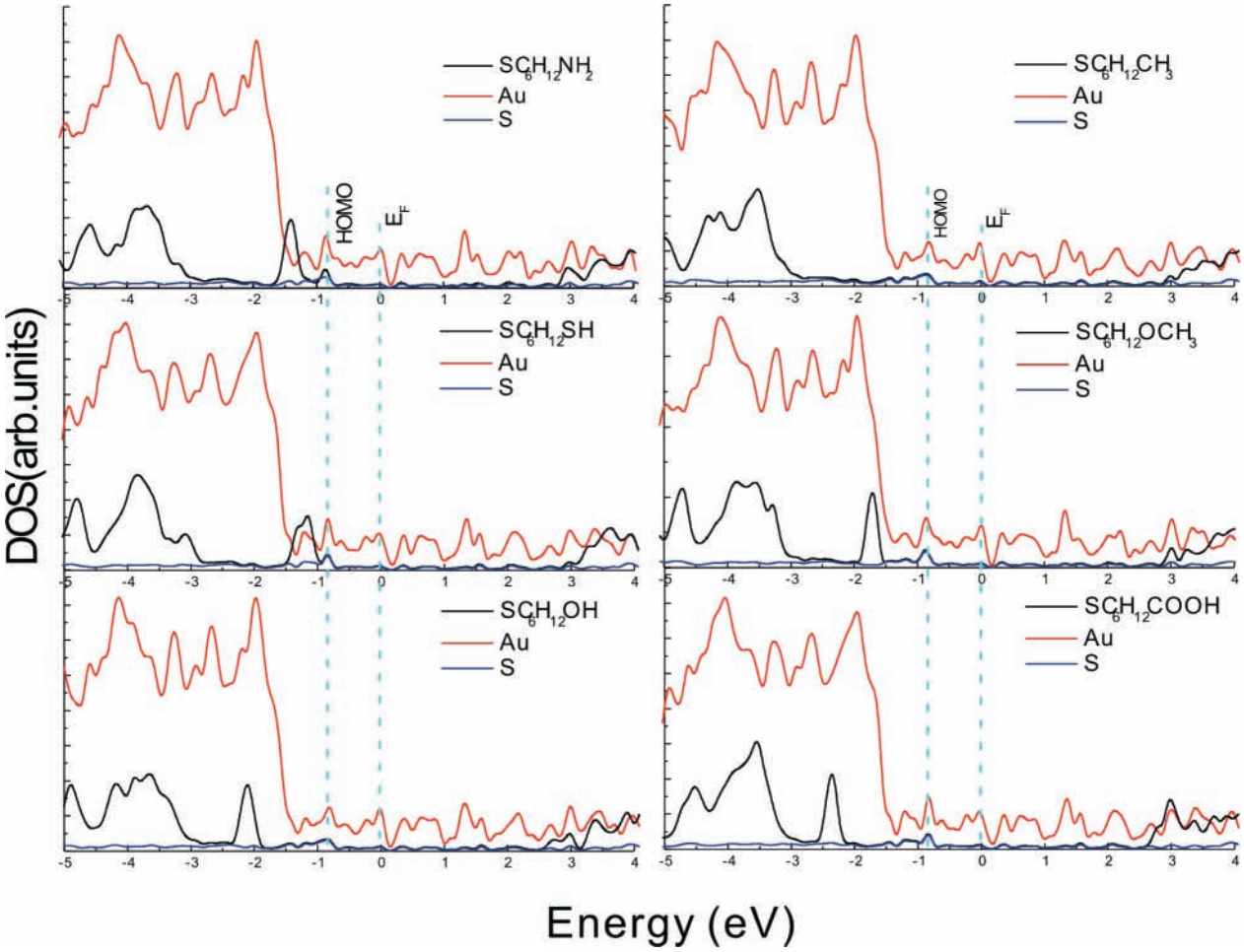

Figure 2. Partial densities of states for $SC_6H_{12}X$ (X = NH_2, SH, OH, CH_3, OCH_3, COOH) monolayers on defect-free Au(111). The dashed vertical blue lines indicate the Fermi energy (which corresponds to our zero energy) and the molecular HOMO, mainly originating from the S head group.

$\Delta\Phi = -1.05$ eV for $SC_6H_{12}CH_3$ monolayers, while a decrease $\Delta\Phi = -1.20$ eV is found for both $SC_6H_{12}OCH_3$ and SC_6H_{12}-COOH; for a more detailed analysis of the origin of the work function changes induced by adsorbed monolayers of thiol molecules, see refs 17, 31, and 32.

Figure 2 shows the computed partial densities of states (PDOS) for monolayers of alkanethiols with different end groups on perfect Au(111). For all adsorbed molecules, the HOMO (which is mainly contributed by the sulfur atom) is found at $\Delta E \sim -0.85$ eV below E_F, independent of the terminal group.[17] This can be rationalized by considering that the structure of the metal−molecule interface, and thus the interface dipole, is the same for all molecules.[17,32] Below the HOMO, a prominent peak appears in the PDOS of all monolayers except SC_6H_{12}-CH_3. This peak, at energy $E_T \sim -1$ to -2.5 eV relative to E_F, originates from states localized on the terminal group itself (see Figure 3), mainly from the lone pairs on the N, S, or O atoms in the end group. At still lower energies, below about -3 eV, the band of occupied states from the alkane chains is present for all adsorbed molecules. The corresponding band of empty states is at energies above ~3 eV, so that E_F is approximately in the middle of the gap between occupied and empty states originating from the alkane chains.

(b) Structure and Electronic Properties of $SC_6H_{12}CH_3$ Monolayers on Au(111) Surfaces Containing Either a Surface Vacancy or an Au Adatom per $\sqrt{3} \times \sqrt{3}$ Unit Cell. Recent studies have provided evidence that alkanethiolate adsorption gives rise to an important restructuring of the Au-(111) surface, with formation of vacancies and/or adatoms.[28,33−36] Motivated by these results, we have considered $SC_6H_{12}CH_3$ monolayers on a defected Au(111) surface that has either one vacancy or one adatom in each $\sqrt{3} \times \sqrt{3}$ surface unit cell. While there is no strict correspondence between the present models and the structures discussed in refs 28, 34, and 35, the present results should provide insights into the effect of adatom and surface vacancies on the electronic structure. On the surface

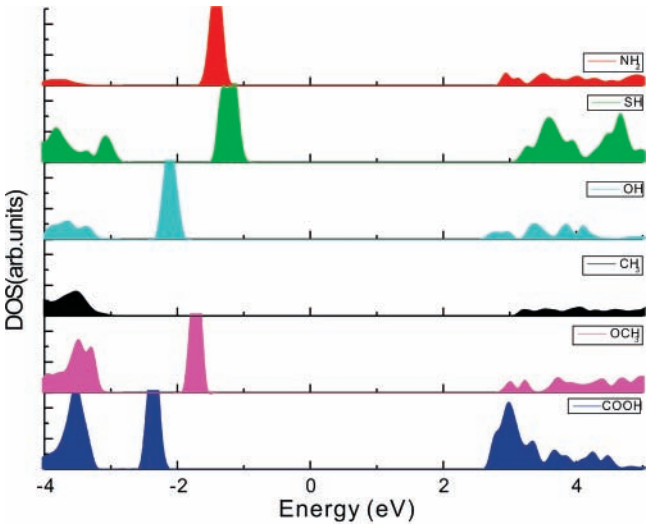

Figure 3. Partial densities of states for the terminal groups of the investigated alkanethiolate monolayers on Au(111).

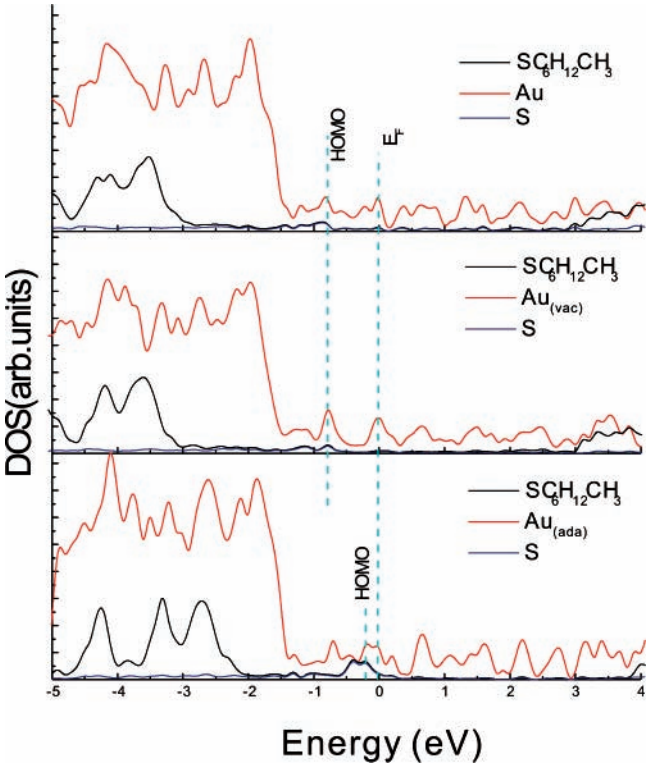

Figure 4. Partial densities of states for $SC_6H_{12}CH_3$ monolayers on perfect Au(111) and Au(111) with vacancies and adatoms. The dashed vertical blue lines indicate the Fermi energy (which corresponds to our zero energy) and the molecular HOMO, mainly originating from the S head group.

with vacancies, the alkanethiol adsorption geometry is very similar to that on the perfect Au(111) surface, with an Au−S bond length of 2.49 Å, whereas on Au(111) with adatoms, the alkanethiols adsorb just on top of the adatoms, and the Au−S bond length, 2.26 Å, is much shorter. Incidentally, the latter adsorption geometry is likely to be similar to that of thiolate and/or dithiolate molecules at break junctions.[37]

Figure 4 compares the PDOS for $SC_6H_{12}CH_3$ monolayers on defect-free and defected surfaces. On Au(111) with vacancies, the position of the HOMO of the adsorbed molecules relative to the Fermi energy E_F of the gold substrate, −0.85 eV, is the same as on the perfect Au(111) surface because the molecules have the same S−Au bonding geometry on the two surfaces. Also, the induced work function modification, $\Delta\Phi = -1.05$ eV, is the same as on perfect Au(111). Instead, on Au(111) with adatoms, the differences in the adsorption structure give rise to corresponding differences in the electronic properties: the HOMO is in this case much closer to E_F, $\Delta E \sim -0.2$ eV, and the induced work function modification is also smaller, $\Delta\Phi = -0.4$ eV (see Table 1).

(c) *I*−*V* Characteristics. The calculated *I*−*V* curves for the investigated $SC_6H_{12}X$ monolayers on defect-free Au(111) are shown in Figure 5a. It appears that *I* depends linearly on *V* at low voltages, with typical values of about 150 pA/molecule in the voltage range between −1 and +1 V. We point out that these values of the tunneling current are $\sim 10^3$ larger than those we reported earlier for similar monolayers,[16,17] in which an incorrect normalization factor was included.[17] From Figure 5a, we also note that the differences in current among the different monolayers are quite significant, up to a factor of ∼3 within the voltage range under consideration, despite the fact that the molecules are all very similar (−alkanethiolates with the same number of methylene units)− and that the metal−molecule

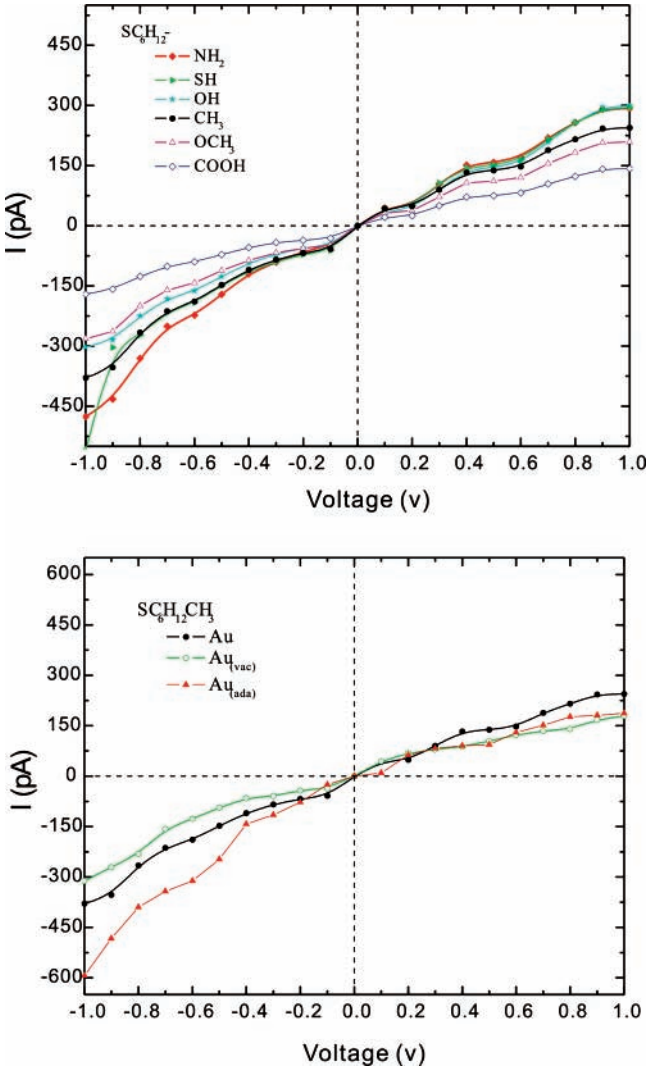

Figure 5. Calculated tunneling current per molecule as a function of the applied bias (see text) for (a) $SC_6H_{12}X$ with different terminal groups (X = NH_2, SH, OH, CH_3, OCH_3, COOH) on defect-free Au(111) and (b) $SC_6H_{12}CH_3$ on perfect Au(111) and on Au(111) surfaces with vacancies (vac) and adatoms (ada).

interface barrier is the same, $|\Delta E| = 0.85$ eV, for the different monolayers. Under both negative (i.e., electrons tunneling from the occupied states of the surface + SAM to the tip) and positive (i.e., electrons tunneling from the tip to the empty states of the surface + SAM) voltages, the SAMs of the -COOH- and -OCH_3 terminated alkanethiols have the smallest conductance, whereas the largest conductance is found for the -SH and -NH_2 terminated molecules. These differences may be related to the combined effect of the work function Φ and the energy E_T of the end group states (see Table 1 and Figure 3), with smaller absolute values of E_T (i.e., peak closer to E_F) and Φ favoring larger currents. In particular, the relative current intensities for the different monolayers are found to scale approximately as the values of $\Phi - E_T$ (= 5.0, 5.4, 5.6, 5.8, and 6.4 eV for -NH_2, -SH, -OH, -OCH_3, and -COOH, respectively). Interestingly, since Φ is largely determined by the dipole field induced by the molecular end group, this amounts to a correlation between the current and the strength of the end group dipole.

Comparison of our results for the *I*−*V* characteristics with available experimental data shows both satisfactory and less favorable aspects. On the positive side, the approximately linear and symmetric appearance of the computed *I*−*V* curves at small voltages agrees well with experiments (see, e.g., ref 10).

Moreover, using the widely accepted value $\beta = \sim 1$ Å^{-1} for the tunneling decay parameter through alkanethiols on gold,[2] we can easily verify that our computed values of the current per molecule, particularly our values for $SC_6H_{12}CH_3$ at 0.2 and 0.5 V (see Table 1), are consistent with most experimental data for somewhat longer alkanethiolate chains with one chemicontact (e.g., SC_8H_{17} and $SC_{10}H_{21}$, see Table 1 in refs 2 and 15). On the less satisfactory side, our results do not agree with recent CP-AFM measurements for SAMs of $SC_6H_{12}X$ with X = CH_3, OH, and NH_2 end groups on Au(111), which found that the average conductance (scaled to 1 nm^2 contact area) for -OH terminated monolayers is about 10 and 100 times larger than for -CH_3 and -NH_2 terminated SAMs, respectively.[30] It should be noted, however, that the structure of the -OH and -NH_2 terminated SAMs was not well-known in ref 30. Thus, we cannot exclude that the observed differences may to some extent originate from a different packing density of the molecules in the different monolayers.

A comparison of the calculated *I*−*V* curves for $SC_6H_{12}CH_3$ on defected and undefected Au(111) is given in Figure 5b. The computed tunneling current intensities for the different cases are similar at positive voltages, whereas a significantly larger current is observed for the defected surface with adatoms under negative bias. This difference can be attributed to the fact that for the Au(111) + adatom surface, the HOMO is much closer to E_F than in the other cases, $\Delta E = -0.18$ versus -0.85 eV, respectively, implying a smaller metal−molecule interface barrier for charge (hole) injection.

Conclusion

In summary, we have studied tunneling through alkanethiolate SAMs on Au(111), forming metal−molecule−tip junctions with a single chemical contact, by means of first principles electronic structure calculations combined with Tersoff−Hamann's theory of the scanning tunneling microscope. The main results of our study are: (i) tunneling currents (*I*) through the investigated SAMs of $SC_6H_{12}X$ molecules depend approximately linearly on low voltages, with typical values of *I* of ∼60 and 150 pA/molecule at 0.2 and 0.5 V, respectively. Despite the simplicity of our approach, and the inherent deficiencies of DFT in describing transport properties,[38] our computed currents per molecule for $SC_6H_{12}CH_3$ agree well with the results of many experimental studies of electrode/SC_nH_{2n+1}/electrode junctions with a single chemicontact.[2,15] (ii) Tunneling currents through SC_6H_{12} X monolayers (X = CH_3, NH_2, SH, OH, COOH, OCH_3) on perfect Au(111) depend remarkably on X, with variations by a factor of ∼3 for voltages in the range of −1 to +1 V. These differences can be related to the accompanying modifications in the work function and terminal partial density of states. In particular, our calculations predict that alkanethiols with -NH_2, -SH, and -CH_3 end groups have larger tunneling conductances than those with -OH, -COOH, and -OCH_3 terminals. (iii) Restructuring of the gold surface via formation of vacancies and adatoms causes changes in the metal−molecule adsorption geometry, which affect the interfacial barrier (lineup of the molecular levels with the metal Fermi energy) and, in turn, the tunneling currents. In particular, a substantially larger tunneling current at negative voltages is found for $SC_6H_{12}CH_3$ bound to an Au adatom. This finding, namely, that the tunneling current depends strongly on the detailed Au−S bonding geometry, agrees with recent observations for molecular junctions involving two chemicontacts.[39] We hope that the results we have presented in this paper will stimulate and/or be useful to future experimental studies.

Acknowledgment. This work was supported by NSF Grant DMR-0213706 to the MRSEC-Princeton Center for Complex Materials. We thank Q. Sun for helpful suggestions and are grateful to G. Scoles for numerous illuminating discussions in the course of the last several years.

References and Notes

(1) Nitzan, A.; Ratner, M. A. *Science (Washington, DC, U.S.)* **2003**, *300*, 1384.
(2) Salomon, A.; Cahen, D.; Lindsay, S.; Tomfohr, J.; Engelkes, V. B.; Frisbie, C. D. *Adv. Mater.* **2003**, *15*, 1881.
(3) Holmlin, R. E.; Haag, R.; Chabinyc, M. L.; Ismagilov, R. F.; Cohen, A. E.; Terfort, A.; Rampi, M. A.; Whitesides, G. M. *J. Am. Chem. Soc.* **2001**, *123*, 5075.
(4) Wold, D. J.; Haag, R.; Rampi, M. A.; Frisbie, C. D. *J. Phys. Chem. B* **2002**, *106*, 2813.
(5) Beebe, J. M.; Engelkes, V. B.; Miller, L. L.; Frisbie, C. D. *J. Am. Chem. Soc.* **2002**, *124*, 11268.
(6) Chabinyc, M. L.; Chen, X.; Holmlin, R. E.; Jacobs, H.; Skulason, H.; Frisbie, C. D.; Mujica, V.; Ratner, M. A.; Rampi, M. A.; Whitesides, G. M. *J. Am. Chem. Soc.* **2002**, *124*, 11730.
(7) Engelkes, V. B.; Beebe, J. M.; Frisbie, C. D. *J. Am. Chem. Soc.* **2004**, *126*, 14287.
(8) Cui, X. D.; Primak, A.; Zarate, X.; Tomfohr, J.; Sankey, O. F.; Moore, A. L.; Moore, T. A.; Gust, D.; Harris, G.; Lindsay, S. M. *Science (Washington, DC, U.S.)* **2001**, *294*, 571.
(9) Wang, W.; Lee, T.; Kretzschmar, I.; Reed, M. A. *Nano Lett.* **2004**, *4*, 643.
(10) Wold, D. J.; Frisbie, C. D. *J. Am. Chem. Soc.* **2001**, *123*, 5549.
(11) Xue, Y.; Datta, S.; Ratner, M. A. *J. Chem. Phys.* **2001**, *115*, 4292.
(12) Di Ventra, M.; Pantelides, S. T.; Lang, N. D. *Phys. Rev. Lett.* **2000**, *84*, 979.
(13) Piccinin, S.; Selloni, A.; Scandolo, S.; Car, R.; Scoles, G. *J. Chem. Phys.* **2003**, *119*, 6729.
(14) Tomfohr, J.; Sankey, O. F. *J. Chem. Phys.* **2004**, *120*, 1542.
(15) Pflaum, J.; Bracco, G.; Schreiber, F.; Colorado, R.; Shmakova, O. E.; Lee, T. R.; Scoles, G.; Kahn, A. *Surf. Sci.* **2002**, *498*, 89.
(16) Liang, J.; Sun, Q.; Selloni, A.; Scoles, G. *J. Phys. Chem. B* **2006**, *110*, 24797.
(17) Sun, Q.; Selloni, A. *J. Phys. Chem. A* **2006**, *110*, 11396.
(18) Tersoff, J.; Hamann, D. R. *Phys. Rev. B* **1985**, *31*, 805.
(19) Perdew, J. P.; Chevary, J. A.; Vosko, S. H.; Jackson, K. A.; Pederson, M. R.; Singh, D. J.; Fiolhais, C. *Phys. Rev. B* **1992**, *46*, 6671.
(20) Fischer, D.; Curioni, A.; Andreoni, W. *Langmuir* **2003**, *19*, 3567.
(21) Vanderbilt, D. *Phys. Rev. B* **1990**, *41*, 7892.
(22) Sandy, A. R.; Mochrie, S. G. J.; Zehner, D. M.; Huang, K. G.; Gibbs, D. *Phys. Rev. B* **1991**, *43*, 4667.
(23) Poirier, G. E. *Langmuir* **1997**, *13*, 2019.
(24) Hayashi, T.; Morikawa, Y.; Nozoye, H. *J. Chem. Phys.* **2001**, *114*, 7615.
(25) Vargas, M. C.; Giannozzi, P.; Selloni, A.; Scoles, G. *J. Phys. Chem. B* **2001**, *105*, 9509.
(26) Gottschalck, J.; Hammer, B. *J. Chem. Phys.* **2002**, *116*, 784.
(27) Fenter, P.; Schreiber, F.; Berman, L.; Scoles, G.; Eisenberger, P.; Bedzyka, M. J. *Surf. Sci.* **1998**, *412*−*413*, 213.
(28) Wang, J.-g.; Selloni, A. *J. Phys. Chem. C* **2007**, *111*, 12149.
(29) Schreiber, F. *Prog. Surf. Sci.* **2000**, *65*, 151.
(30) Gosvami, N.; Lau, K. H. A.; Sinha, S. K.; O'Shea, S. J. *Appl. Surf. Sci.* **2006**, *252*, 3956.
(31) Renzi, V. D.; Rousseau, R.; Marchetto, D.; Biagi, R.; Scandolo, S.; Pennino, U. D. *Phys. Rev. Lett.* **2005**, *95*, 46804.
(32) Heimel, G.; Romaner, L.; Bredas, J. L.; Zojer, E. *Phys. Rev. Lett.* **2006**, *96*.
(33) Molina, L. M.; Hammer, B. *Chem. Phys. Lett.* **2002**, *360*, 264.
(34) Maksymovych, P.; Sorescu, D. C.; Yates, J. T., Jr. *Phys. Rev. Lett.* **2006**, *97*, 146103.
(35) Mazzarello, R.; Cossaro, A.; Verdini, A.; Rousseau, R.; Casalis, L.; Danisman, M. F.; Floreano, L.; Scandolo, S.; Morgante, A.; Scoles, G. *Phys. Rev. Lett.* **2007**, *98*, 16102.
(36) Yu, M.; Bovet, N.; Satterley, C. J.; Bengio, S.; Lovelock, K. R. J.; Milligan, P. K.; Jones, R. G.; Woodruff, D. P.; Dhanak, V. *Phys. Rev. Lett.* **2006**, *97*, 166102.
(37) Chen, F.; Li, X.; Hihath, J.; Huang, Z.; Tao, N. *J. Am. Chem. Soc.* **2006**, *128*, 15874.
(38) Toher, C.; Filippetti, A.; Sanvito, S.; Kieron, B. *Phys. Rev. Lett.* **2005**, *95*, 146402.
(39) Venkataraman, L.; Klare, J. E.; Tam, I. W.; Nuckolls, C.; Hybertsen, M. S.; Steigerwald, M. L. *Nano Lett.* **2006**, *6*, 458.